PAPER

Formation of long- and short-periodic nanoripples on stainless steel irradiated by femtosecond laser pulses

To cite this article: Shuangshuang Hou *et al* 2011 *J. Phys. D: Appl. Phys.* **44** 505401

IOP PUBLISHING JOURNAL OF PHYSICS D: APPLIED PHYSICS

J. Phys. D: Appl. Phys. **44** (2011) 505401 (7pp) doi:10.1088/0022-3727/44/50/505401

Formation of long- and short-periodic nanoripples on stainless steel irradiated by femtosecond laser pulses

Shuangshuang Hou[1], Yanyan Huo[1], Pingxin Xiong[1], Yi Zhang[1], Shian Zhang[1], Tianqing Jia[1,3], Zhenrong Sun[1], Jianrong Qiu[2] and Zhizhan Xu[2]

[1] State Key Laboratory of Precision Spectroscopy, Department of Physics, East China Normal University, Shanghai 200062, People's Republic of China

[2] State Key Laboratory of High Field Laser Physics, Shanghai Institute of Optics and Fine Mechanics, Shanghai 201800, People's Republic of China

E-mail: tqjia@phy.ecnu.edu.cn

Received 27 June 2011, in final form 8 November 2011
Published 2 December 2011
Online at stacks.iop.org/JPhysD/44/505401

Abstract

In this paper, we report the formation of long-periodic (LP) ripples with a period of 530–600 nm and short-periodic (SP) ripples with a period of 260–320 nm on stainless steel irradiated by 800 nm femtosecond laser pulses. The split of LP ripples plays the decisive role in the formation of SP ripples. We further conduct pump-probe experiments and numerical simulations to study the ultrafast dynamics of the formation of surface periodic ripples.

(Some figures may appear in colour only in the online journal)

1. Introduction

Laser-induced periodic ripples on semiconductors have been studied intensely in the last four decades. The periods of surface ripples induced by long-pulse lasers are usually close to the laser wavelength λ. These periodic ripples are attributed to the interference between the incident laser and the surface scattered light field [1–3]. Recently, nanoripples with periods significantly smaller than λ have been observed in semiconductors and dielectrics after the irradiation of linearly polarized femtosecond laser pulses. In order to understand the mechanisms of the formation of surface ripples, several explanations have been proposed, such as self-organization, enhancement of the local electric field in nanoplasmas and laser–plasmon interference [4–14]. The formation mechanism of periodic surface ripples induced by femtosecond laser pulses is an interesting and confusing problem, on which more experimental and theoretical studies should be conducted. In recent years, the formation of long-periodic (LP) ripples on metals induced by femtosecond laser pulses has attracted considerable attention. Guo *et al* studied the ultrafast dynamics of the formation of surface ripples on Cu, Ag and Au. They found that the surface patterns on Cu were much clearer than those on Au, which was attributed to the much higher electron–phonon coupling coefficient in Cu [15]. They also studied the evolution of the LP ripples on platinum and gold. They proposed that the decrease in the ripple periods was attributed to the increase in the effective refractive index in the air–metal interface when the periodic ripples become deeper and regular [16]. Huang *et al* studied the formation of LP ripples on CuZn, and proposed that the periodic ripples originated from the interference between the surface plasmons and incident laser [17]. In addition to the LP ripples, Namba's group reported the formation of short-periodic (SP) ripples on stainless steel irradiated by femtosecond laser pulses [18]. As pointed out in this reference, more experiments need to be carried out to give more insight into the formation mechanisms of SP ripples on metals.

Metallic nanostructures can support surface plasmon resonances. The resonant wavelength and the local field enhancement depend sensitively on their geometrical shapes [19–22]. These metallic nanostructures have attracted intensive interest for their important roles in the nanophotonic field, such as local surface plasmon resonance shift,

[3] Author to whom any correspondence should be addressed.

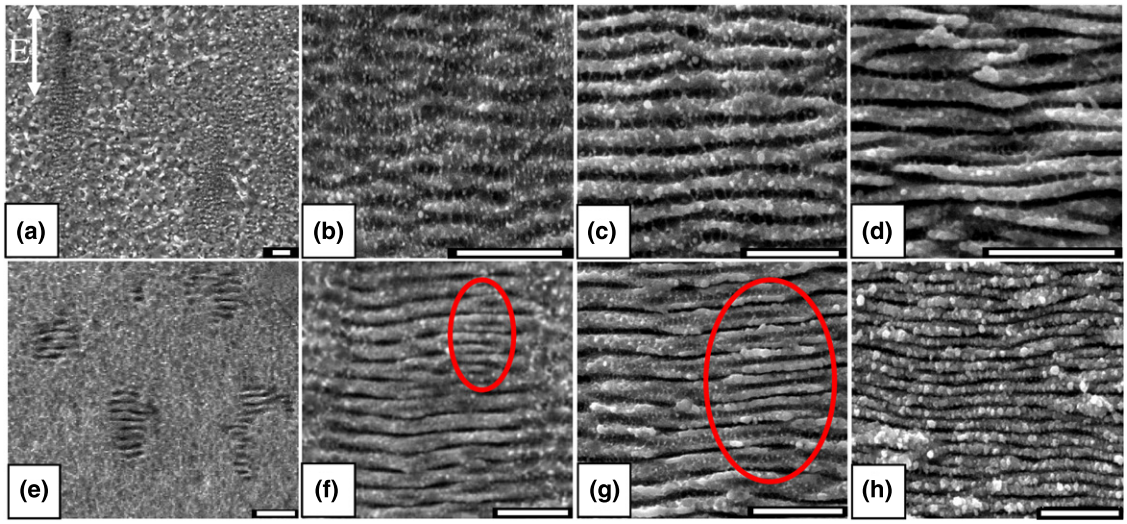

Figure 1. SEM images of the surface patterns by the laser irradiation at fluences of (*a*)–(*d*) 0.16 J cm^{-2} and (*e*)–(*h*) 0.07 J cm^{-2}. The irradiation pulse numbers are (*a*) 10, (*b*) 50, (*c*) 100, (*d*) 500, (*e*) 95, (*f*) 180, (*g*) 400 and (*h*) 1000, respectively. E direction shows the laser polarization, and the scale bar is 2 μm.

surface-enhanced Raman scattering and infrared absorption [23–25]. Recently, Guo *et al* reported the formation of LP ripples on aluminium and platinum, and found that the formation of surface periodic ripples changed the optical properties obviously [26, 27]. By adjusting the laser fluence and pulse number, green, golden and black aluminium films were fabricated. The optical absorption of blackened metals of Pt and NiTi was enhanced to 85–95% [28–30]. Meanwhile, after LP ripples formed on the surface of a tungsten lamp filament, its emission efficiency was enhanced by 100% [31]. Laser-induced periodic nanostructures provide a new method for changing the metallic optical properties for various purposes, and have great potential applications in solar energy and optical sensitive elements [32]. In this paper, we study the formation of LP and SP ripples on stainless steel irradiated by 800 nm femtosecond laser pulses. Our experimental results show that the split of LP ripples plays the decisive role in the formation of SP ripples. We conduct pump-probe experiments and numerical simulations to study the ultrafast dynamics of the formation of LP and SP ripples.

2. Experimental setup

The experiment is conducted on a commercial Ti : sapphire regenerative amplifier laser system (Legend Elite, Coherent). It generates laser pulses at a centre wavelength of 800 nm with a pulse duration of 50 fs and pulse energy of 3.5 mJ. The laser system operates at a repetition rate of 1–1000 Hz. The laser beam goes through a lens with a focal length of 250 mm, and irradiates on the sample surfaces (stainless steel). We place the samples at the position of 32 mm in front of the laser focus. The diameter of the laser spot on the sample surface is 500 μm, hence in the observation area with size less than $50 \times 50\ \mu\text{m}^2$, the laser intensity is uniform. A half-wave plate and a Glan polarizer are used to change the laser power continuously, and an electronic shutter to control the irradiation pulse numbers. The samples are mounted on a *XYZ*-translation stage controlled by a computer. After the laser irradiation, the sample is dipped in pure water, and cleaned by an ultrasonic cleaner for 10 min to remove the plume dust deposited on the ablation area.

The pump-probe experimental setup is similar to that described in [11]. The laser beam is split into a pump and a probe beam with a power ratio of 93 : 1. The probe beam goes through a delay line and simultaneously confocal with the probe one on the sample surface. The sample surface is monitored with a microscope and a CCD camera, which ensures that the confocal error is less than 10 μm. The temporal zero point is measured by the sum frequency at 400 nm via a BBO crystal. The reflected pulse energy is measured by an energy meter, and total reflection is acquired.

3. Results and discussion

3.1. Formation of LP and SP ripples

By controlling the laser fluence and irradiation pulse number, we fabricated two kinds of periodic ripples on stainless steel: LP ripples with periods of 600–400 nm and SP ripples with periods of 310–270 nm, as shown in figures 1 and 2. From figures 1(*a*) and (*e*), we find that shallow ripples emerge in local areas, which is attributed to the interference coupling between the surface plasmon and the incident laser. For the normal incident laser, the plasmonic wavelength at the metal/dielectric interface is given by [33]

$$\lambda_s = \lambda((\varepsilon_{r1} + \varepsilon_d)/\varepsilon_{r1}\varepsilon_d)^{1/2}. \quad (1)$$

ε_d is the dielectric constant of air ($\varepsilon_d \approx 1$), and ε_{r1} is the real part of the dielectric constant of metal and λ is the wavelength of the incident laser ($\lambda = 800$ nm). After the shallow ripples form on the metal surface, the coupling between the surface plasmon and the incident laser will be enhanced, and the laser field localizes in the groove [17]. Figure 1(*c*) clearly shows that the ripples become deeper and regular, and their

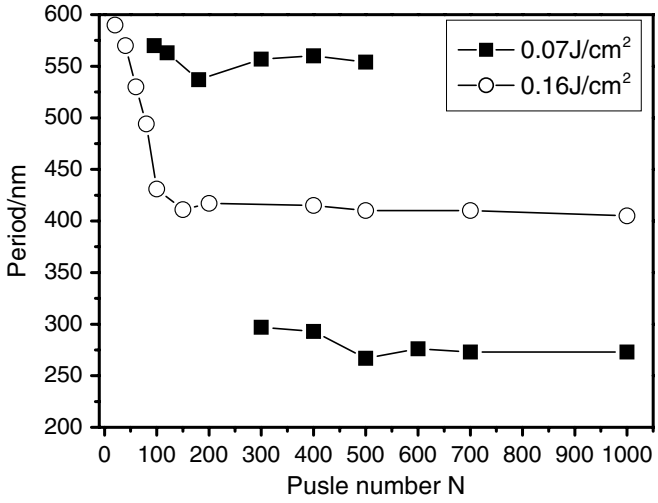

Figure 2. Dependence of ripple period on the pulse number N.

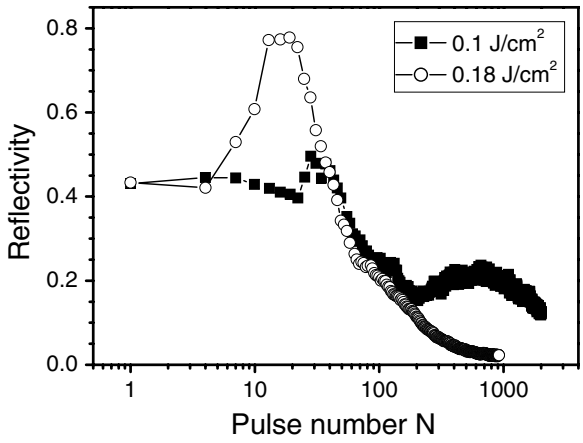

Figure 3. Reflectivity with the probe pulse number N at $\Delta t = 0$ ps.

periods decrease to 490 nm. As the pulse number increases to 500, the periods decrease to 410 nm. Figure 2 shows that during irradiation of the initial 180 laser pulses, the periods decrease rapidly from 600 to 410 nm. Hereafter, they only fluctuate at the value of 410 nm. Reference [18] also showed that the periods decreased with the deepening of gratings. Moreover, the plume in the plasma state ejected from the laser spot will increase the dielectric constant of air in the neighbouring region, and this also reduces the ripples' periods [17]. These are the two reasons that make the period decrease rapidly in the initial 180 pulses, as shown in figure 2. However, the accumulation thermal effects will induce a thick melted layer. It prevents further deepening of grooves as well as further increasing of the electric field intensity there [17, 18]. Therefore, the periods approach a constant value, which explains well the results shown in figure 2.

However, for the incident laser with a fluence of 0.07 J cm^{-2}, as periodic ripples formed on a partial area of the irradiated region, the periods do not decrease with increasing laser pulse, which is shown clearly in figure 2. Meanwhile, we observed an interesting phenomenon of the split of LP ripples, as shown in red circles of figures 1(f) and (g). The SP ripples grew rapidly and formed on the whole ablation area after being irradiated by 600 pulses. The split of LP ripples plays the dominant role in the formation of SP ripples.

We further study the formation of periodic surface ripples irradiated by lasers with different laser fluences. The results indicate that when laser fluence F is less than 0.05 J cm^{-2}, no surface ripples are observed on the sample surface even when irradiated by 10 000 pulses. If laser fluence F is increased to 0.13 J cm^{-2}, LP ripples begin to split after irradiation by 50 pulses, and the ripple period approaches 300 nm after being irradiated by 400 pulses. Namely, regular SP ripples form on the ablation area if the laser fluences change in the range 0.07–0.13 J cm^{-2}. When the laser fluences are higher than 0.15 J cm^{-2}, only LP ripples can be observed on the sample surface.

3.2. Results of pump-probe experiment

In the pump-probe experiment, the delay time is adjusted to be 0 ps, and their polarizations are parallel [11]. Figure 3 shows the dependences of reflectivity on the pulse number. For a laser fluence of 0.18 J cm^{-2}, the reflectivity does not change during the irradiation of initial four pulses. Part of the pulse energy begins to get deposited in the sample, but there is no clear ablation spot. The reflectivity increases rapidly after irradiation by 5–20 laser pulses. This is because the high-density surface plasma is excited and the sample begins to be ablated. The reflectivity then begins to decrease rapidly because of the growth of LP ripples for diffraction and light localization. After irradiation by 200 pulses, the reflectivity decreases to values less than 10%.

In figure 3, we have eliminated the error caused by the diffraction of pump laser after the surface ripples formed, because it is only 5% of the probe signal.

If laser fluence decreases to 0.1 J cm^{-2}, the reflectivity increases at most by 5%, which means only low-density surface plasma forms on the stainless steel surface. With the surface ripples growing longer and deeper, the reflectivity decreases to a value less than 15% as the pulse number N increases to 200. The reflectivity then slightly increases to 22% with further laser pulse irradiation. After 2000 pulses irradiation, the reflectivity decreases to 10%.

For a laser fluence of 0.1 J cm^{-2}, the reflectivity increases only by 5%, which is much less than the value of $F = 0.18$ J cm^{-2}, by 35%. Furthermore, the reflectivity increases twice for $F = 0.1$ J cm^{-2} and only once for $F = 0.18$ J cm^{-2}.

4. Theoretical calculation

4.1. Theoretical model

The reflection coefficient of a metal surface is given by [34]

$$R = \frac{(n-1)^2 + k^2}{(n+1)^2 + k^2}. \qquad (2)$$

Table 1. Relative dielectric constants and plasma parameters used in the theoretical calculation.

F (J cm^{-2})	ε_{r1}	ε_{r2}	ω_p(rad s^{-1})	Γ(rad s^{-1})
0	−4.4	22.3i	2.33×10^{16}	9.74×10^{15}
0.07	−2.01	18.55i	2.55×10^{16}	1.45×10^{16}
0.16	−2.31	125.1i	1.62×10^{17}	8.9×10^{16}

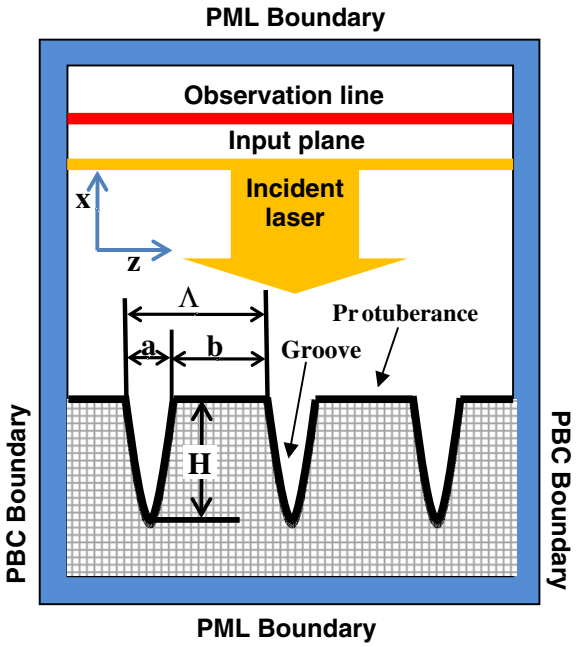

Figure 4. The model of FDTD simulation.

In equation (2), $n = \sqrt{(\sqrt{\varepsilon_{r1}^2 + \varepsilon_{r2}^2} + \varepsilon_{r1})/2}$, $k = \sqrt{(\sqrt{\varepsilon_{r1}^2 + \varepsilon_{r2}^2} - \varepsilon_{r1})/2}$. By measuring λ_s and R, we can calculate the real (ε_{r1}) and imaginary (ε_{r2}) parts of the relative dielectric constants using equations (1) and (2). If the incident laser fluence is 0.07 J cm^{-2}, $\lambda_s = 570$ nm and $R = 54.6\%$ are measured, and for a laser fluence of 0.16 J cm^{-2}, $\lambda_s = 602$ nm and $R = 78\%$. The calculated relative dielectric constants are shown in table 1.

The dielectric function of stainless steel is described by the Drude model [34]:

$$\varepsilon_r(\omega) = \varepsilon_{r1} + i\varepsilon_{r2} = \varepsilon_\infty - \omega_p^2/\omega(\omega + i\Gamma). \quad (3)$$

In equation (3), ω is the laser frequency. Plasma frequency $\omega_p = (1/2\pi c)(4\pi Ne^2/m\varepsilon_\infty)^{1/2}$, where N is the density of free electrons, which changes with the electric field E, and $\Gamma$is the electron collision frequency, which can be derived from the data ε_{r1} and ε_{r2}. The calculated results and the starting state of the stainless steel surface are also shown in table 1.

The commercial software OPTIFDTD was used to calculate the electric field intensity and the reflectivity. The shape of the ripple grooves was observed by an atomic force microscope (AFM) in [17], so we choose the parabolic shape as the ripple groove shape. The model is shown in detail in figure 4. We also calculate the cases of different shapes, such as square and trapezoidal shapes, and the phenomena are similar to each other. The incident laser is a Gaussian beam with a radius of 10 μm, and its central wavelength is at 800 nm and its polarization in the z direction. The groove depth and width are shown as H and a, and the period as Λ. We take the periodic boundary conduction (PBC boundary) in the z direction, and the perfect match layer (PML boundary) in the x direction. The reflected light is collected on the observation line.

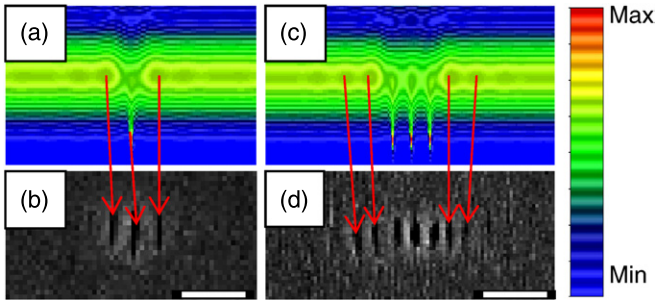

Figure 5. Electric field distribution in the surface of stainless steel with one groove (a), (b) and three grooves (c), (d). The scale bar is 2 μm.

4.2. Ultrafast dynamics of the formation of LP and SP ripples

If there are subwavelength apertures on the metallic surface, the surface plasmon will be excited. The interference between surface plasmons and incident laser induces the formation of periodic ripples. Figure 5(a) shows the electric field on the sample surface with a groove of 100 nm width and 60 nm depth. The laser field localizes in the groove and its two sides, and two more grooves will be induced there, as shown in figure 5(b). If there are three grooves with a period of 560 nm on the sample surface, figure 5(c) shows that the interference between surface plasmons and incident laser field is enhanced, and more periodic ripples will be induced in the neighbouring area (see figure 5(d)). With increasing laser pulse number, more and more periodic ripples form on the sample surface (see figures 1(e) and (f)). In the calculation of figure 5, the plasma frequency is taken as $\omega_p = 2.55 \times 10^{16}$ rad s^{-1} and the electron collision frequency is $\Gamma = 1.45 \times 10^{16}$ rad s^{-1}. An absorption boundary in the z direction is used.

Figures 1–3 show that if the laser fluences are less than 0.13 J cm^{-2}, the LP ripples will split into two SP ripples and the reflectivity increases twice with the irradiation of laser pulse. Figures 6 and 7 present the evolution of the electric field intensity and reflectivity with groove depth. The simulation model is shown in figure 4. Here the period is taken as 560 nm, and the groove width is 100 nm. The dielectric constants are the same as those in figure 5. The electric field intensity I_1 in the groove is obviously higher than the value on the protuberance I_2. Therefore, the groove becomes deeper rapidly. The deepening of the grooves will, inversely, enhance the electric field intensity in the groove itself, while I_2 and the reflectivity Ref decrease. This is a positive feedback process [17]. However, when the groove is deeper than 120 nm, I_1 approaches its maximum value of 2.6, and I_2 and the reflectivity Ref begin to increase. The incident laser begins

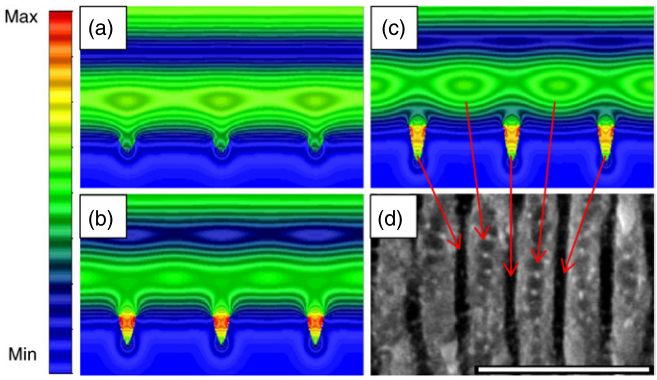

Figure 6. Electric field intensity for groove depths of (*a*) 50, (*b*) 120, (*c*) 160 nm and (*d*) SEM image of the surface pattern. The scale bar is 2 μm.

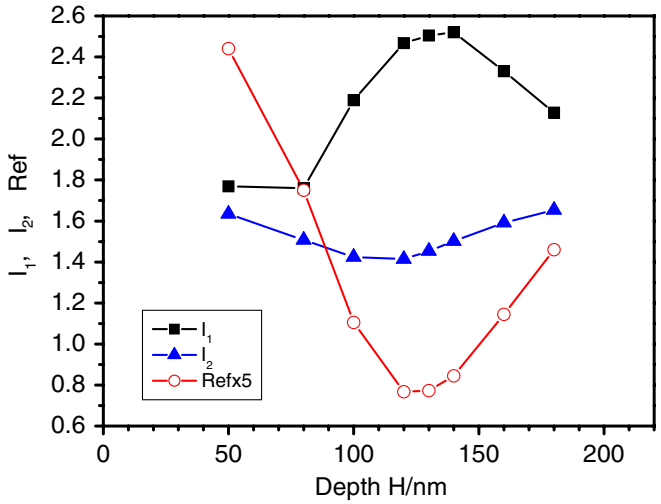

Figure 7. Electric field intensity in the groove I_1, on the protuberance I_2, and the reflectivity Ref as functions of groove depth.

to localize on the protuberance, as shown in figure 6(*c*), and I_2 becomes rather strong as the depth increases to 160 nm. Correspondingly, figure 6(*d*) shows that new shallow grooves appear on the protuberances.

Keeping the depth of the old groove as 160 nm and width as 100 nm, we study the changes of the electric field intensities in the two grooves with depth h of the new ones. The SEM image shown in figure 6(*d*) indicates that at the beginning, the new groove is rather wide, and the laser can be very easily localized there, as shown in figure 8(*b*). Figure 8(*c*) shows that the electric intensity I_{new} in the new grooves increases rapidly with depth, and it will exceed the value in the old one as its depth is larger than 60 nm. This will induce the split of LP ripples and the formation of SP ripples (shown as figures 8(*b*) and (*d*)). In the meantime, the reflectivity increases with the formation of SP ripples, which fits well with the pump-probe experimental results. In the calculation, the plasma frequency is taken as $\omega_p = 2.55 \times 10^{16}$ rad s^{-1} and the electron collision frequency is $\Gamma = 1.45 \times 10^{16}$ rad s^{-1}.

When the plasma frequency is taken as $\omega_p = 1.62 \times 10^{17}$ rad s^{-1} and the electron collision frequency as $\Gamma = 8.9 \times 10^{16}$ rad s^{-1}, we find, however, that the laser field cannot be localized on the protuberance even if the groove depth increases to 160 nm. Figure 9 shows that the electric field intensity in the groove is enhanced by a factor of 4, namely the light intensity is as strong as 16 times the incident laser. The strong coupling between the surface plasma and the incident laser induces a surface shape resonance for groove depth changing in a rather larger region, and the incident laser is nearly totally localized in the grooves [35].

In order to understand the difference in the electric field intensity on the protuberance between the two cases for the plasma frequency taken as $\omega_p = 1.62 \times 10^{17}$ rad s^{-1} and $\omega_p = 2.55 \times 10^{16}$ rad s^{-1}, we further calculate the electric field intensity on the periodic surface of dielectrics. In the grooves, I_1 is always less than 2 and no localization can be formed on the protuberance. Therefore, the strong light localization in the grooves and on the protuberance comes mainly from the surface plasmon.

On the surface with a low-density plasma ($\omega_p = 2.55 \times 10^{16}$ rad s^{-1}), the distribution of electric field intensity is in the internal states between the above two cases. In the grooves, I_1 is only enhanced by a factor of 2 even for the surface shape resonance. When the groove depth is larger than 120 nm, it is out of the surface shape resonance, and the electric field will distribute in the regions out of the grooves [35], for example, on the protuberance. As light localizes on the protuberance, it induces a new groove there, and further induces the split of LP ripples.

We have made similar experiments on CuZn and Al. However, only LP ripples were observed [15–17]. No SP ripples formed in the ablation area, even after irradiation by thousands of laser pulses. It is believed to be caused by the different dielectric constants of CuZn, Al and stainless steel. Our calculation results indicate that if the coupling between the surface plasmon and the incident laser is very strong, the laser field is localized mainly in the grooves, rather than on the protuberance. Therefore, no splitting of the LP ripples occurs.

The periods of LP ripples increase with the laser wavelengths [17, 36], and the SP ripples' periods increase correspondingly, too. However, as discussed in [15], the thermal effects significantly influence the formation of periodic surface ripples. For ultraviolet laser pulses, we think the SP ripple period is too short to form easily.

5. Conclusions

In this paper, we report the formation of long- and short-periodic ripples on stainless steel irradiated by 800 nm femtosecond laser pulses. The results indicate that if the laser fluence $F > 0.15$ J cm^{-2}, only LP ripples can be observed. If laser fluences change in the range 0.07–0.13 J cm^{-2}, regular LP and SP ripples form in sequence on the laser spot. The split of LP ripples plays a decisive role in the formation of SP ripples. Pump-probe experimental results show that for a laser fluence of 0.18 J cm^{-2}, the reflectivity increases to 79% after irradiation by tens of laser pulses and decreases to a value less than 10% after irradiation by hundreds of laser pulses. For a laser fluence of 0.07 J cm^{-2}, the reflectivity increases twice. We make a theoretical calculation to study

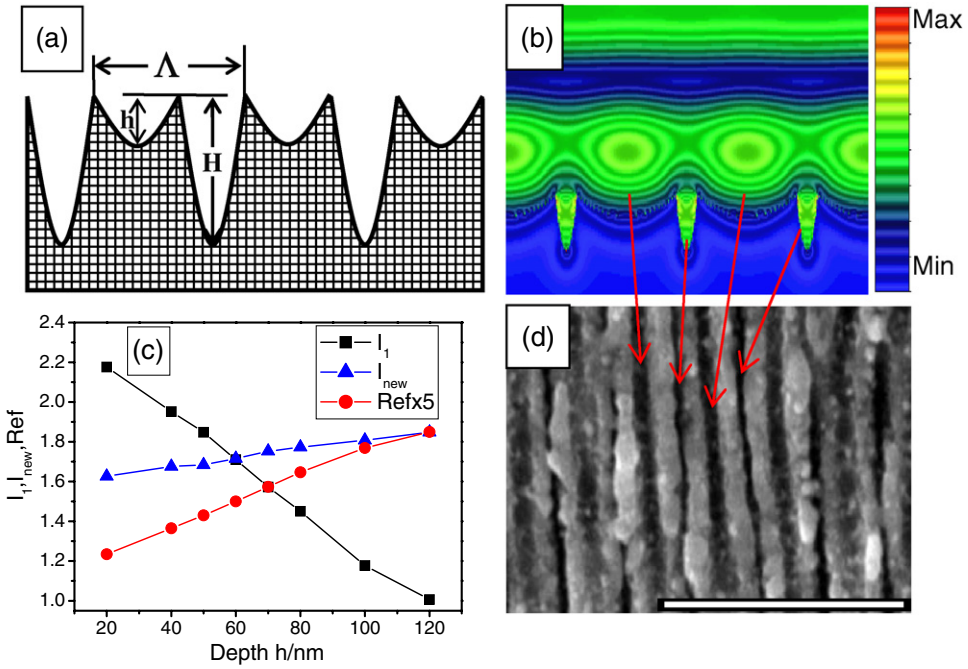

Figure 8. (*a*) Surface structures with new and old grooves, (*b*) electric field intensity on the surface with the depth of new groove of 60 nm, (*c*) dependences of I_1, I_{new} and Ref on the depths of the new grooves, and (*d*) SEM image. The scale bar is 2 μm.

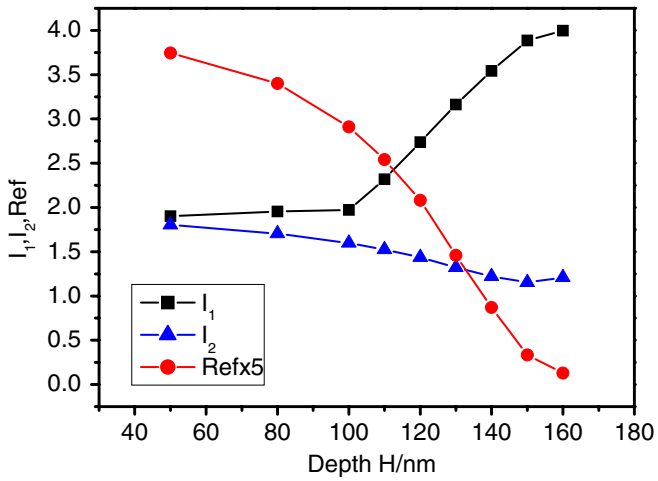

Figure 9. Electric field intensity in the groove I_1, on the protuberance I_2, and the reflectivity Ref as functions of groove depth.

the ultrafast dynamics of the formation of LP and SP ripples. If the surface layer is in high-density plasma states ($\omega_p = 1.62 \times 10^{17}$ rad s^{-1}), the strong coupling of the incident laser and the surface plasmons induce the laser energy to be highly localized in the grooves. The deepening of the grooves and the coupling between the surface plasmons and the incident laser are positive feedback processes, and induce the formation of LP ripples. While for the surface layer in low-density plasma states ($\omega_p = 2.55 \times 10^{16}$ rad s^{-1}), the coupling between surface plasmons and incident laser is weaker, and the laser is only weakly localized in the grooves. When it is out of the surface shape resonance as the groove is too deep, the light is localized on the protuberance between two grooves. This induces the split of LP ripples. We also study the evolution of reflectivity during the formation of LP and SP ripples, and explain well the pump-probe experimental results.

Acknowledgments

This work is supported by the National Natural Science Foundation of China (10874044, 11004060 and 10904038), the National Special Science Research Program of China (2011CB808105 and 2010CB923203), the Shanghai Municipal Science and Technology Commission (09JC1404700, 10JC1404500 and 09ZR1409300) and the Twilight Project (07SG25).

References

[1] Birnbaum M 1965 Semiconductor surface damage produced by Ruby laser *J. Appl. Phys.* **36** 3688
[2] Emmony D C, Howson R P and Willis L J 1973 Laser mirror damage in germanium at 10.6 μm *Appl. Phys. Lett.* **23** 598
[3] Young J F, Preston J S, van Driel H M and Sipe J E 1983 Laser-induced periodic surface structure. Experiments on Ge, Si, Al, and brass *Phys. Rev.* B **27** 1155
[4] Costache F, Henyk M and Reif J 2002 Modification of dielectric surfaces with ultra-short laser pulses *Appl. Surf. Sci.* **186** 352
[5] Shimotsuma Y, Kazansky P G, Qiu J R and Hirao K 2003 Self-organized nanogratings in glass irradiated by ultrashort light pulses *Phys. Rev. Lett.* **91** 247405
[6] Bhardwaj V R, Simova E, Rajeev P P, Hnatovsky C, Taylor R S, Rayner D M and Corkum P B 2006 Optically produced arrays of planar nanostructures inside fused silica *Phys. Rev. Lett.* **96** 057404
[7] Shen M, Carey J E, Crouch C H, Kandyla M, Stone H A and Mazur E 2008 High-density regular arrays of nanometer-scale rods formed on silicon surfaces via femtosecond laser irradiation in water *Nano Lett.* **8** 2087

[8] Dufft D, Rosenfeld A, Das S K, Grunwald R and Bonse J 2009 Femtosecond laser-induced periodic surface structures revisited: a comparative study on ZnO *J. Appl. Phys.* **105** 034908
[9] Juodkazis S, Nishimura K and Misawa H 2007 In-bulk and surface structuring of sapphire by femtosecond pulses *Appl. Surf. Sci.* **253** 6539
[10] Huang M, Zhao F L, Cheng Y, Xu N S and Xu Z Z 2009 Mechanisms of ultrafast laser-induced deep-subwavelength gratings on graphite and diamond *Phys. Rev.* B **79** 125436
[11] Miyaji G and Miyazaki K 2006 Ultrafast dynamics of periodic nanostructure formation on diamondlike carbon films irradiated with femtosecond laser pulses *Appl. Phys. Lett.* **89** 191902
[12] Jia X, Jia T Q, Ding L E, Xiong P X, Deng L, Sun Z R, Wang Z G, Qiu J R and Xu Z Z 2009 Complex periodic micro-/nanostructures on 6H-SiC crystal induced by the interference of three femtosecond laser beams *Opt. Lett.* **34** 788
[13] Jia X, Jia T Q, Zhang Y, Xiong P X, Feng D H, Sun Z R, Qiu J R and Xu Z Z 2010 Periodic nanoripples in the surface and subsurface layers in ZnO irradiated by femtosecond laser pulses *Opt. Lett.* **35** 1248
[14] Borowiec A and Haugen H K 2003 Subwavelength ripple formation on the surfaces of compound semiconductors irradiated with femtosecond laser pulses *Appl. Phys. Lett.* **82** 4462
[15] Wang J C and Guo C L 2005 Ultrafast dynamics of femtosecond laser-induced periodic surface pattern formation on metals *Appl. Phys. Lett.* **87** 251914
[16] Vorobyev A, Makin V and Guo C L 2007 Periodic ordering of random surface nanostructures induced by femtosecond laser pulses on metals *J. Appl. Phys.* **101** 034903
[17] Huang M, Zhao F, Cheng Y, Xu N and Xu Z Z 2009 Origin of laser-induced near-subwavelength ripples: interference between surface plasmons and incident laser *ACS Nano* **3** 4062
[18] Qi L, Nishii K and Namba Y 2009 Regular subwavelength surface structures induced by femtosecond laser pulses on stainless steel *Opt. Lett.* **34** 1846
[19] Prodan E, Radloff C, Halas N J and Nordlander P 2003 A hybridization model for the plasmon response of complex nanostructures *Science* **302** 419
[20] Wang H, Brandl D W, Nordlander P and Halas N 2007 Plasmonic nanostructures: artificial molecules *Acc. Chem. Res.* **40** 53
[21] Stewart M E, Anderton C R, Thompson L B, Maria J, Gray S K, Rogers J A and Nuzzo R G 2008 Nanostructured plasmonic sensors *Chem. Rev.* **108** 494
[22] Anker J N, Hall W P, Lyandres O, Shah N C, Zhao J and Van Duyne R P 2008 Biosensing with plasmonic nanosensors *Nature Mater.* **7** 442
[23] Willets K A and Van Duyne R P 2007 Localized surface plasmon resonance spectroscopy and sensing *Annu. Rev. Phys. Chem.* **58** 267
[24] Kneipp K 2007 Surface enhanced Raman scattering *Phys. Today* **60** 40
[25] Jensen T R, Van Duyne R P, Johnson S A and Maroni V A 2000 Surface-enhanced infrared spectroscopy: a comparison of metal island films with discrete and nondiscrete surface plasmons *Appl. Spectrosc.* **54** 371
[26] Vorobyev A and Guo C L 2008 Colorizing metals with femtosecond laser pulses *Appl. Phys. Lett.* **92** 041914
[27] Dusser B, Sagan Z, Soder H, Faure N, Colombier J P, Jourlin M and Audouard E 2010 Controlled nanostructures formation by ultrafast laser pulses for color marking *Opt. Express* **18** 2913
[28] Vorobyev A Y and Guo C L 2008 Femtosecond laser blackening of platinum *J. Appl. Phys.* **104** 053516
[29] Vorobyev A Y, Topkov A N, Gurin OV, Svich V A and Guo C L 2009 Enhanced absorption of metals over ultrabroad electromagnetic spectrum *Appl. Phys. Lett.* **95** 121106
[30] Yang Y, Yang J J, Liang C Y and Wang H S 2008 Ultra-broadband enhanced absorption of metal surfaces structured by femtosecond laser pulses *Opt. Express* **16** 11259
[31] Vorobyev AY, Makin V S and Guo C L 2009 Brighter light sources from black metal: significant increase in emission efficiency of incandescent light sources *Phys. Rev. Lett.* **102** 234301
[32] Vorobyev A Y and Guo C L 2007 Effects of nanostructure-covered femtosecond laser-induced periodic surface structures on optical absorptance of metals *Appl. Phys.* A **86** 321
[33] Raether H 1988 *Surface Plasmons on Smooth and Rough Surfaces and on Grating* (Berlin: Springer)
[34] Markovic M I and Rakic A D 1990 Determination of the reflection coefficients of laser light of wavelengths $\lambda \in (0.22\mu\text{m}, 200\mu\text{m})$ from the surface of aluminum using the Lorentz–Drude model *Appl. Opt.* **29** 24
[35] López-Rios T, Mendoza D, García-Vidal F, Sánchez-Dehesa J and Pannetier B 1998 Surface shape resonances in lamellar metallic gratings *Phys. Rev. Lett.* **81** 665
[36] Vorobyev A Y and Guo C L 2008 Femtosecond laser-induced periodic surface structure formation on tungsten *J. Appl. Phys.* **104** 063523